Electrical Conductivity of 1:1 and 2:1 Clay Minerals

A. Kriaa[a], M. Hajji[b], F. Jamoussi[b], and A. H. Hamzaoui[b]

[a]*Ecole supérieure des Sciences et Techniques de Tunis, Département de Physique Chimie, 5 avenue Taha Hussein, 1008 Montfleury, Tunis, Tunisia, e-mail: Kriaa1993@Yahoo.fr*
[b]*Centre National de Recherches en sciences des Matériaux, Laboratoire de Valorisation des Matériaux Utiles, Borj Cedria, BP 95, 2050, Hammam lif, Tunis*

The A.C. impedance plots were used as tools to analyze the electrical response of two varieties of Tunisian halloysite 1:1 and illitic samples 2:1 as a function of frequency at different temperatures (80–800°C). The real and imaginary parts of the complex impedance trace semicircles in the complex plane. Except for the illite, It-1, the second sample analyzed in this study, these plots give evidence for the presence of both bulk and grain boundary effect, above 600°C onwards. The bulk resistance of the materials decreases with the rise in temperature. Impedance Spectroscopy data reveal a non-Debye type of dielectric relaxation. The Nyquist plots show the negative temperature coefficient of resistance of both pure Tunisian illite and halloysite samples. The results of bulk electrical conductivity and its activation energy are presented for the two mineral clay samples. For illite It-1, the activation energy values estimated from the AC conductivity pattern and modulus pattern are very similar and suggest a possibility of a long-range mobility of charge carriers (ions) via hopping mechanism of electrical transport processes at higher temperature. On the other hand, for the halloysite sample provided from kasserine, (Ha-Kass), the modulus analysis admit that the electrical transport processes of the material are very likely of electronic nature. Relaxation frequencies follow an Arrhenius behavior with the activation energy values not comparable to those found for the electrical conductivity.

Keywords: kaolinite, illite, hopping mechanism, impedance analysis, electrical conductivity.

УДК 550.832

INTRODUCTION

The electrical conductivity and dielectric permittivity (commonly named as dielectric constant ε), of the constituent minerals are the main controlling factors of the electrical properties of soils. The dielectric permittivity of a material is a measure of the relative ability to store a charge (electrical energy) for a given applied electric field while dielectric loss is a measure of the proportion of the charge transferred in conduction and stored in polarization. The dielectric constant ε is a complex number and is a function frequency. The relative dielectric constant $\varepsilon^*(\omega)$ is the ratio of the complex dielectric constant ε to dielectric constant of free space ε_0. The real part of the dielectric constant of soils particles is between 3 and 6 whereas that of water is 80 at 20°C [1, 2]. Thus the dielectric constant of soil-water mixture is between 4 and 8 depending on the proportion of each. Clay minerals are an important constituent of many mineral soils. The influence they may have on the dielectric behavior of a moist soil is therefore of great importance [3].

Ionic conductivity is known to occur in clay minerals and to be an important contributor to dielectric dispersion. The amount of conduction is related to the surface density of charge and the surface area. In general, the halloysite 1:1 clay mineral has a relatively small surface area and low ion-exchange capacity and would be expected to be associated with a low ionic conductivity, while the interlayers of the 2:1 clay minerals provide space into which cations can be adsorbed. In illite clays the interlayer contains potassium which fixes the structure rigidly. On the other hand, a large surface area of the smectite compared with other clay minerals, its capacity to swell and its ability to adsorb ions means it should create a reasonably electrically conductive material. It should be pointed out that the electrical properties of clays are still unknown at large in literature. In fact these materials are difficult to handle and experimental data are very limited. There are some literature data concerning electrical properties of clay and sandstone [4], clay or mixtures of sand/clay [5–6], conductivity measurements of dry clay minerals conducted at different temperatures in the range from 80 to 800°C have not been widely studied so far. Most of the articles published on the AC conductivity of rocks investigate the effect of water or oil content [7, 8] but no studies report on the characterization of the microstructure of clays as ceramic materials by analyzing their electrical conductivities in the range of temperatures cited above. Obviously this study could be useful for Na-conducting materials.

Meanwhile, Impedance Spectroscopy (IS) is a relatively mature, cheap, and simple technique for non-destructive testing, which has been widely used to characterize the electrical properties of the materials and relate the changes in these electrical properties to microstructural changes occurring in the materials. Recently, growing interest has been developed in employing IS to characterize the microstructure of ceramic materials [9–11] particularly for

studying the microstructure evolution in cement during hydration and hardening [12–14]. There are many ways IS data may be plotted. In the IS field, where capacitive rather than inductive effects dominate, conventionally one plots – Im (Z) ≡ -Z'' on the y-axis vs. Re (Z) ≡ Z' on the x-axis to give a complex-plane impedance plot. Such graphs have been usually termed Nyquist plots. They have the disadvantage of not indicating frequency response directly, but may nevertheless be very helpful in identifying conduction processes present. Another approach, the Bode diagram, is to plot log [|Z|] and Φ ~ vs. log [f]. Alternatively, one can plot Z' (or any I') or -Z'' (or -I''), or the logs of these quantities vs. log [f] [15, 16].

In this paper, we report details concerning the physico-chemical characterization study of two Tunisan kaolinite (Ka.Kass) and illite (It-1) clays mineral providing from north and south west of Tunisia, respectively. The main goal is to present We present also a complete analysis about electrical properties of these two clay mineral samples using impedance spectroscopy technique at different temperatures ranging from 80 to 800°C. The characterization of the microstructure of Na-conducting ceramics is probably useful by this electrochemical technique. In the case of many mineral complex solid, the analysis of IS data, when depicted in a complex plane plot, appears generally in the form of a succession of semicircles representing the contributions to the electrical properties due to the bulk material, grain boundary effects and interfacial polarization phenomena if any. Taking into account these properties, the analysis of electric modulus enables us to separate the effects due to each component (bulk, grain boundary, and electrode polarization effects) in a solid sample very easily.

MATERIALS AND METHODS

Clays

Sample of specimen halloysite 1:1 clay used in this study provided from Touila, in Kasserine (Ha-Kass) situated at the north west of Tunisia. It is important to notice that this solid sample is on natural pure state, of white color and with no impurities. Whereas, the other clay sample chosen in this study, is the It-1 illite 2:1 clay, a pure Tunisian illite (light green) from the south west. For the two samples particles with diameter < 45 μm were obtained by sedimentation and saturated with Na^+ by 7 washing cycles (successive centrifugal treatments) with 1M NaCl. After each centrifugation of the suspension, the supernatant was discarded and replaced with fresh solution of NaCl. After that, the samples were dialysed through a specific membrane, oven dried to a constant mass at 80°C and finally stored in an air-tight container prior to use.

Sample Clay Characterisation

X-ray diffraction (XRD)

X-ray diffractograms were recorded using a "PANalytical X'Pert HighScore Plus" diffractometer with the radiation $K\alpha_1$ of copper. Two types of diffractograms are studied: diffractograms with disorientated powder where all the lines (h, k, l) appear, and diffractograms of oriented plate obtained by sedimentation. This makes it possible to follow the periodicity of the stratification of the layers, with the reflection (001) on which the identification is based.

Cation Exchange Capacities (CEC) and Specific Surface Areas (SSA)

CEC was determined by the method of copper ethylendiamine $(EDA)_2\,CuCl_2$ complex analogous to that described by Bergaya and Vayer [17]**.** A known volume (2 to 5 ml) of the 0,05M $Cu(EDA)_2^{2+}$ solution (prepared firstly by mixing 1M$CuCl_2$ with an excess 1M EDA) is diluted with water to 25 ml and added to the clay (0,4 g) in the centrifuge tube and the pH of suspension is determined. The suspension is shaken or stirred for 30 min to ensure complete exchange, centrifuged and the pH is determined once more. The concentration of the Cu $(EDA)_2^{2+}$ remaining in the solution was determined by atomic absorption spectroscopy (AAS) or iodometry. The CEC of the sample can be obtained by the difference in Cu concentration in the initial and final solutions as determined by AAS or iodometry and the CEC calculated from the quantity of absorbed Cu $(EDA)_2^{2+}$ (amount initially added to the clay minus amount remaining).

A specific surface area BET was determined by nitrogen gas adsorption at 77K, using a "Quantachrom-Autosorb1" sorptiometer.

X-ray patterns

The specimens after different treatments were studied by using X-ray diffraction technique. In these methods, oriented specimen is prepared on glass microscope slides. The samples were successively subjected to different treatments not only to characterize the clay specimens but to identify the presence of interstratified or mixed other clay minerals:

i) Normal at ambient temperature (N);

ii) Saturated with ethylene glycol (EG-treatment) (G);

iii) Heating at 550°C (H).

The diffractogram of the illite It-1 sample is shown on the Fig. 1. In the patterns of the air-dried

oriented mount of pure It-1(*N*), the basal reflections of illite appear along with an irrational series of reflections: $d_{(001)}$ reflection at 10.08 Å, the $d_{(002)}$ at 5.01 Å and the $d_{(003)}$ at 3.31 Å. The XRD patterns of the EG-treated (*G*) and heated specimens (*H*) at 550°C were included in the Fig. 1 in order to detect minimal changes. One can observe that these peaks are not affected by treatments, i.e., the illite basal reflections do not show significant changes.

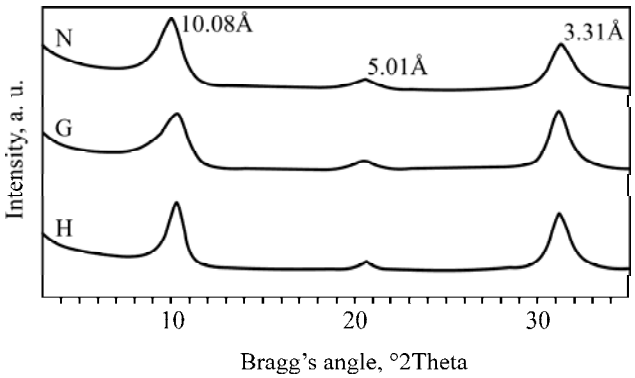

Fig. 1. XRD patterns of oriented purified clay plate illite It-1 (*N*: Normal, *H*: Heated 550°C, *G*: saturated by ethylene glycol).

The XRD pattern of the Kasserine clay (Ha-Kass) (Fig. 2) shows sharp peaks at d = 10.01 Å, 4.40 Å, 3.34 Å and 2.58 Å attributed to the halloysite $4H_2O$ clay mineral that belongs to kaolin group [18]. When heated at 550°C, these peaks disappear.

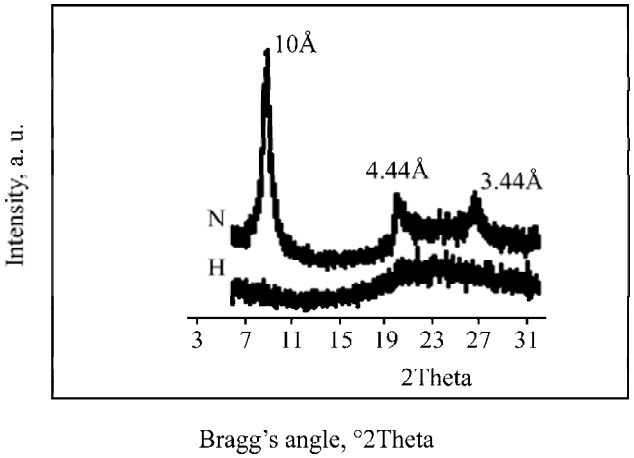

Fig. 2. XRD of purified Ha-Kass and heated at 500°C.

The cation ion-exchange capacity (CEC) and the Specific Surface Area (SSA) of the clay samples are reported in Table 1.

Table 1. C.E.C and S.S.A for two studied clay samples.

Specimen	CEC (meq/100g)	SSA (m^2/g)
It-1	27	45
Ha-Kass.	39.84	24.57

Chemical analyses and structural formulas

The clay samples were attacked by a mixture of three acids (HCl, H_2SO_4, HNO_3). All the elements pass in solution, except the silica (SiO_2) which is determined by gravimetry. Other elements, such as Al, Fe, Mg, Ca, Na and K are assayed by an Atomic Absorption Spectrophotometer (AAS).

The chemical analysis of clay mineral samples is given in Table 2. The loss on ignition value of the Ka-Kass clay is relatively very important (28.96%); it can be due to the presence of a supplementary water layer.

Table 2. Chemical analyses of fractions of purified mineral clays.

Weight %	SiO_2	Al_2O_3	Fe_2O_3	MgO	Na_2O	K_2O	CaO	Ignition loss
It-1	50.24	24.38	5.58	2.13	1.21	9.39	0.05	7.53
Ha.Kass	39.40	29.91	0.19	0.27	0.52	0.1	0.65	28.96

It follows from these analyses that the average structural formulas are:

$$\text{It-1: } K_{1.64}Ca_{0.01}Na_{0.32}\,[Si_{6.89}Al_{1.11}]^{IV}\,[Al_{2.82}Fe_{0.57}Mg_{0.44}]^{VI}\,O_{20}(OH)_4.$$

$$\text{Ha-Kass: } Na_{0.17}K_{0.02}Ca_{0.11}\,[Si_{6.49}Al_{1.51}]^{IV}\,[Al_{4.239}Fe_{0.024}Mg_{0.07}]^{VI}\,O_{22}.$$

It reveals that the studied samples presented two significant substitutions in the octahedral and tetrahedral layers. For illite It-1the potassium (K) and metal (M) ions are present to satisfy the negative charge and will not be used in the calculation of negative charge. Thus net layer charge of illite It-1 per unit cell is 1.97 charge/cell whereas for Ha-Kass is 0.3 charge/cell.

For electrical conductivities studies, the finely ground samples were pressed into cylindrical pellets of 10–13 mm diameter and 1mm thickness using a hydraulic press at a pressure of 6 000 Kg/cm^2. The pellets were mounted between two flat silver electrodes in an evacuated conductivity setup and annealed at 100°C for 24h to avoid adsorbed water. The AC impedance data, the modulus of impedance $|Z|$ and phase angle were obtained in the frequency range 1Hz to 13 MHz using HP4192A controlled frequency response analyzer over the temperature range 80–800°C. Before measurements, an input AC signal of voltage amplitude ~ 10 mV was applied across the sample cell followed by thermal stabilization for half an hour. The temperature of the sample was controlled by means of a temperature controller (West Model 6100) with an accuracy of ± 1°C. A computer with serial cable RS232 and software Labview 4.0 have been used for data acquisition.

RESULTS AND DISCUSSION

Impedance studies

A polycrystalline material usually gives grain boundary properties with different time constants leads to two successive semi-circles. The electrical properties of a material are often represented in

terms of some complex electrical parameters like complex permittivity ε*, electric modulus *M** and dielectric loss tan δ. They are related to each other as follows:

Complex impedance,

$$Z^* = Z' - jZ'' = R_s - 1/j\omega C_s. \quad (1)$$

Complex permittivity,

$$\varepsilon^* = \varepsilon' - j\varepsilon'', \; tan\,\delta = \varepsilon''/\varepsilon'. \quad (2)$$

Complex modulus,

$$M^* = M' + jM'' = jwC_0Z^*. \quad (3)$$

Where R_s is the series resistance, $\omega = 2\pi f_r$ (f_r = resonance frequency), C_s the capacitance in series, $j = (-1)^{1/2}$ the imaginary factor and C_0 is the vacuum capacitance of the circuit elements. Above four expressions give a wide scope for graphical representation.

On the other hand, the peak of the high frequency semi-circular arc in the impedance spectrum enables us to evaluate the relaxation frequency (ω_{max}) of the bulk material in accordance with the relation

$$\omega_{max}\,\tau = R_bC_b = 1 \text{ or}$$
$$2\pi f_{max}\,R_bC_b = 1 \Rightarrow f_{max} = 1/2\pi R_bC_b \quad (4)$$

and

$$\tau = 1/\,2\pi f_{max} \quad (5)$$

where R_b and C_b refer to bulk resistance and capacitance, respectively, τ represents relaxation time and $\omega = 2\pi f$ is the angular frequency. Besides, the bulk conductivity (σ) of the material is a thermally activated process obeying Arrhenius behavior. It is calculated in accordance with the relation

$$\sigma = (\sigma_0/T)\exp(-Ea/kT). \quad (6)$$

From expression (2), the complex permittivity

$$\varepsilon^* = \varepsilon' - i\varepsilon''$$

where ε' is the real or relative permittivity or dielectric constant and; ε'', the imaginary or dielectric loss, ε* can be represented as [19].

$$\boldsymbol{\varepsilon^*} = 1/j\omega C_0Z^* \quad (7)$$

where C_0 is the capacitance of free space. The ε' real and ε'' imaginary parts of dielectric permittivity were calculated from impedance data of illite IMt-1 and kaolinite Ka-kass clay minerals, measured over a range 1 Hz to 13 MHz at different temperatures using

$$\boldsymbol{\varepsilon'} = (t/A\omega\varepsilon_0)[Z''/(Z'^2+Z''^2)] \quad (8)$$

$$\boldsymbol{\varepsilon''} = (t/A\omega\varepsilon_0)[Z'/(Z'^2+Z''^2)] \quad (9)$$

It must be noticed that ε' and ε'' represent, respectively, the dielectric constant and the dielectric loss of the material.

From expression (3), the complex electric modulus *M** is the reciprocal of the complex permittivity ε*

$$M^* = 1/\boldsymbol{\varepsilon^*} \quad (10)$$

where

$$M' = (A/t)\omega\varepsilon_0Z'' \text{ and } M'' = (A/t)\omega\varepsilon_0Z'. \quad (11)$$

The σ_{AC} was calculated using the measured impedance data of studied clay samples over a frequency range of 1 Hz to 13 MHz at different selected temperatures using

$$\boldsymbol{\sigma_{AC}} = (t/A)[Z'/(Z'^2 + Z''^2)] \quad (12)$$

where *t* is the thickness and *A* the area of the sample pellet.

Impedance spectrum analysis

First, it must be pointed out that the impedance spectra measured at temperatures above 400°C are reproducible. But at temperatures below 400°C, several factors could affect impedance measurements, e.g. incomplete contact between sample and electrode, short circuit through a less resistive path in clay, and the presence of moisture in clay.

The electrical behavior of the system has been studied over a range of frequency and temperature using AC technique of IS. The plot of -Z'' versus Z' (so called Nyquist plot) of It-1 at different temperatures (400–800°C) is shown in Figs. 3a–c.

One can observe that the effect of temperature on impedance behavior of the material sample becomes clearly visible with rise in temperature (Figs. 3a–c). The impedance spectrum is characterized by the appearance of single semicircular arc whose pattern of evolution changes with rise in temperature (Figs. 3a-b). Each semicircular arc in the impedance pattern can be attributed to a parallel combination of resistance and capacitance. The center of the semicircular arc shifts towards the origin on increasing temperature which indicates that the conductivity of the illite It-1 increases with increase in temperature. With further rise in temperature, appearance of another semicircular arc in the impedance spectrum has been noticed on and after 600°C. The pattern is displayed in Fig. 3c. The presence of a single semicircular arc up to 595°C indicates that the electrical processes in the material arise basically due to the contribution from bulk material (grain interior) [20–22] and can be modeled as an equivalent electrical circuit comprising of a parallel combination of bulk resistance (R_b) and bulk capacitance (C_b). The electrical process at these temperatures may be attributed to intragrain phenomena.

Appearance of additional semicircular arcs in the impedance pattern with increasing in temperature ($T \geq 600$°C) indicates the beginning of intergranular

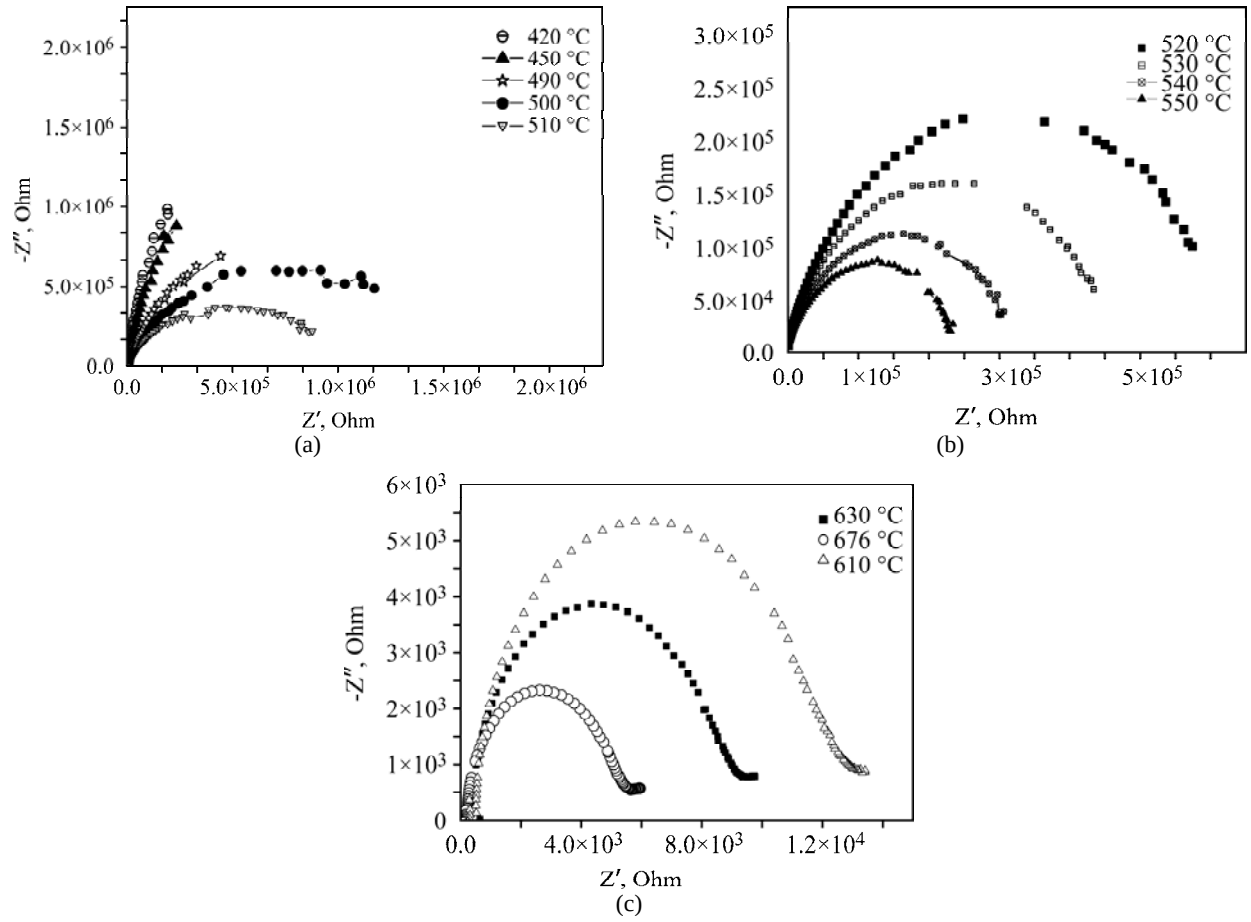

Fig. 3. Impedance spectra as a function of temperature for illite It-1 sample.

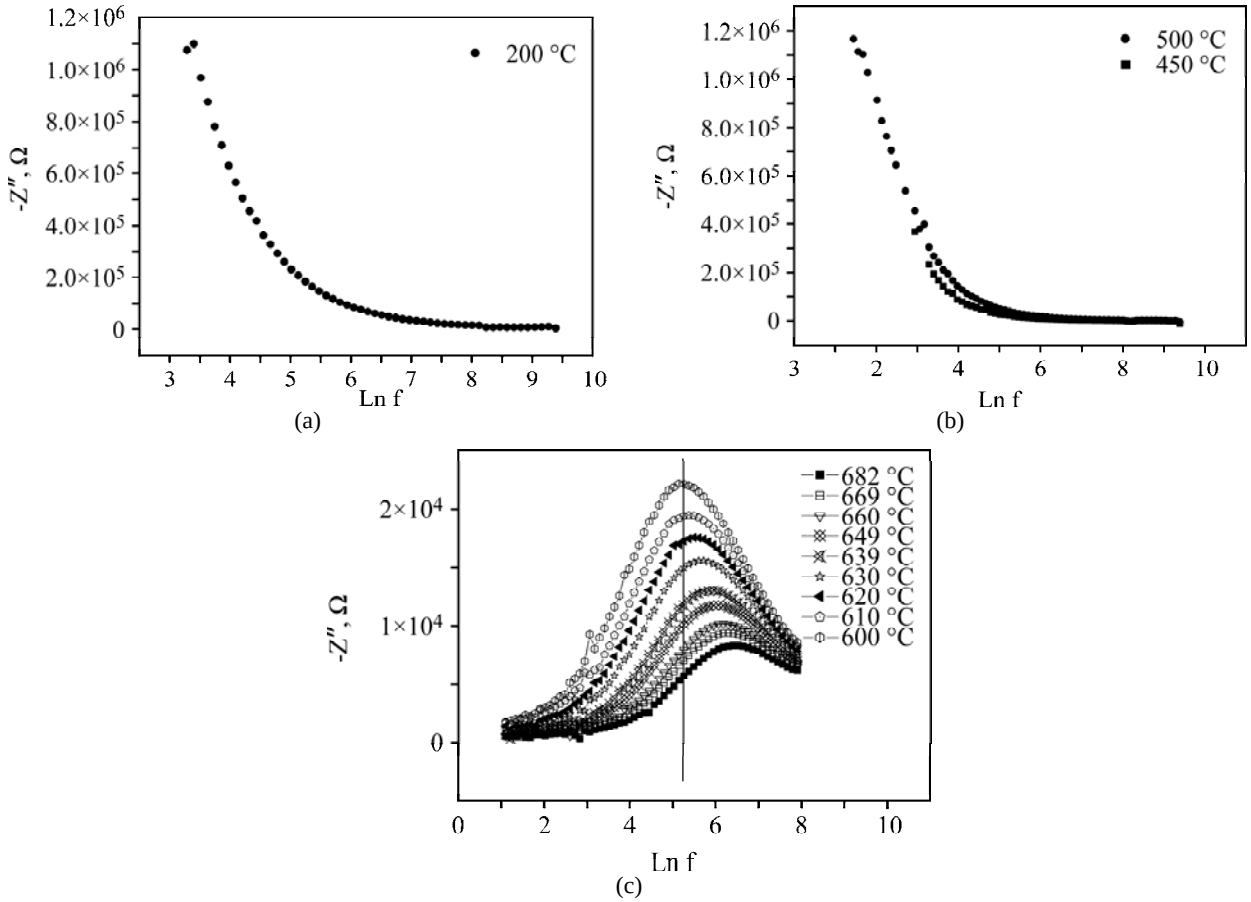

Fig. 4. Variation of imaginary part of impedance (*Z*") as a function of frequency for illite It-1**.**

activities within the clay sample with definite contributions from both bulk (grain interior) and grain boundary effects (Figs. 3b–c). This type of electrical phenomena in the material can appropriately be modeled in terms of an equivalent electrical circuit, according to brick layer model [23], comprising of a series combination of two parallel R-C circuits attributed to both the grain interior (bulk) and grain boundary effects in agreement with Brahma et al [22].

Figs. 4a–c show the loss spectrum i.e. variation of the imaginary part of the impedance (*Z*'' with frequency at different temperatures.

We must emphasis that when temperature is between $200 \leq t \leq 450$°C, a monotonous decrease in (*Z*'') without any peak in the frequency range (ii) appearance of peaks in the loss spectrum (iii) typical peak broadening with increase in temperature and (iv) asymmetric peak broadening. The absence of peaks up to a temperature 450°C in the pattern indicates negligible or absence of current dispersion in this temperature region. Fig. 4c shows peaks at unique frequency that describes the type and strength of electrical relaxation phenomenon in the material [22, 24]. A significant broadening of the peaks with increasing in temperature suggests the presence of electrical processes in the material [25]. In addition, the coincidence of the impedance *Z* values at higher frequencies at all the temperatures indicates a possible release of space charge.

Figs. 5a–c show the variations of real part of impedance (*Z*' i.e. bulk resistance) with frequency at different temperatures.

As we can observe, at relatively low temperature (up to 500°C), the curve *Z*' vs. *ln f* shows a monotonic de crease in the value of *Z*' with temperature. The impedance value is typically higher at lower temperatures in the low-frequency region and decreases gradually with increasing frequency (Fig. 5b). As the temperature increases, the pattern of variation of *Z*' as a function of frequency assumes a sigmoidal variation in the low–frequency region follow by a plateau region at higher frequency. This behavior has been observed to be almost similar at temperatures on and above 530°C (Figs. 5c and d). In addition the magnitude of *Z*' a (bulk resistance) decreases with increasing temperature in the low-frequency ranges and appears to merge in the high–frequency region irrespective of temperature. This result can be attributed to the release of space charge as a result of reduction in the barrier properties of the clay mineral sample as already mentioned in other works by some authors [22, 25, 26]. The same authors have emphasized that this phenomenon may be a responsible factor for the enhancement of AC conductivity of material with temperature at higher frequencies.

Electrical conductivity analysis

The conductivity $\sigma(\omega)$ has been evaluated from complex impedance spectrum data. Fig. 6 shows the variation of $\sigma(\omega)$ as a function of temperature.

This plot indicates a linear increase of conductivity with rise in temperature with a typical Arrhenius-type behavior in two domains, having linear dependence of logarithm of conductivity Ln ($\sigma \times T$) on inverse of temperature $10^3/T$ K^{-1}, i.e., the electrical conductivity is a thermally process, and obeys the Arrhenius law $\sigma = (\sigma_0/T) \exp(-Ea/kT)$ where the symbols have their usual meanings. The activation energy (*Ea*) of the clay mineral sample can be calculated from the slope of a straight line. The increasing of conductivity with rise in temperature shows a typical characteristic of a semiconductor (i.e., negative temperature coefficient of resistance-type behavior). This curve indicates the presence of two slopes in the pattern $\sigma(\omega)$ vs. $10^3/T$ corresponding respectively to activation energy values $Ea_1 = 0.95$ eV and $Ea_2 = 2.07$ eV, situated at the temperature range between 570 and 580°C. This is attributed very likely to a change in the conduction mechanism, leading to an increase of the ionic conduction resulting either to a decrease of the barrier to ion motion or to a decrease of the number of mobile ions. Anyway, this could not be ascribed to a phase transition in the material, i.e. to a structural change since this structural change does not occur for the illite sample between 500–600°C. In fact, most of the studies described in the literature concerning the DTA curves of illitic samples show an endothermic reaction between 500–600°C which is characteristic of the nonexpendable three-layer type of clay minerals [27]. Illite could only dehydroxylate in this temperature range.

Fig. 7 shows the variation of Log σ versus log (*f*) at various temperatures for illite It-1. It is observed that the frequency dependence of conductivity shows two distinct regimes, within the measured frequency window: i) the low frequency plateau region and; ii) high frequency dispersion region. The plateau region corresponds to frequency independent conductivity (σ_{DC}) and dispersion region corresponds to the frequency–dependent part (σ_{AC}). The σ_{DC} value could be obtained by extrapolating the conductivity value to the zero limit frequency.

The observed frequency dependent conductivity can be described by the equation of Jonscher (1983) [28]: $\sigma(\omega) = \sigma_{DC} + A\omega^n$, where n is the frequency exponent in the range of $0 < n < 1$, a and *n* are thermally activated quantities, hence electrical conduction is a thermally activated process. The *AC* conductivity (σ_{AC}) was found to obey the power law $A\omega^n$ ($n < 1$). The value of *n* was 7.65×10^{-5} at $T = 600$°C.

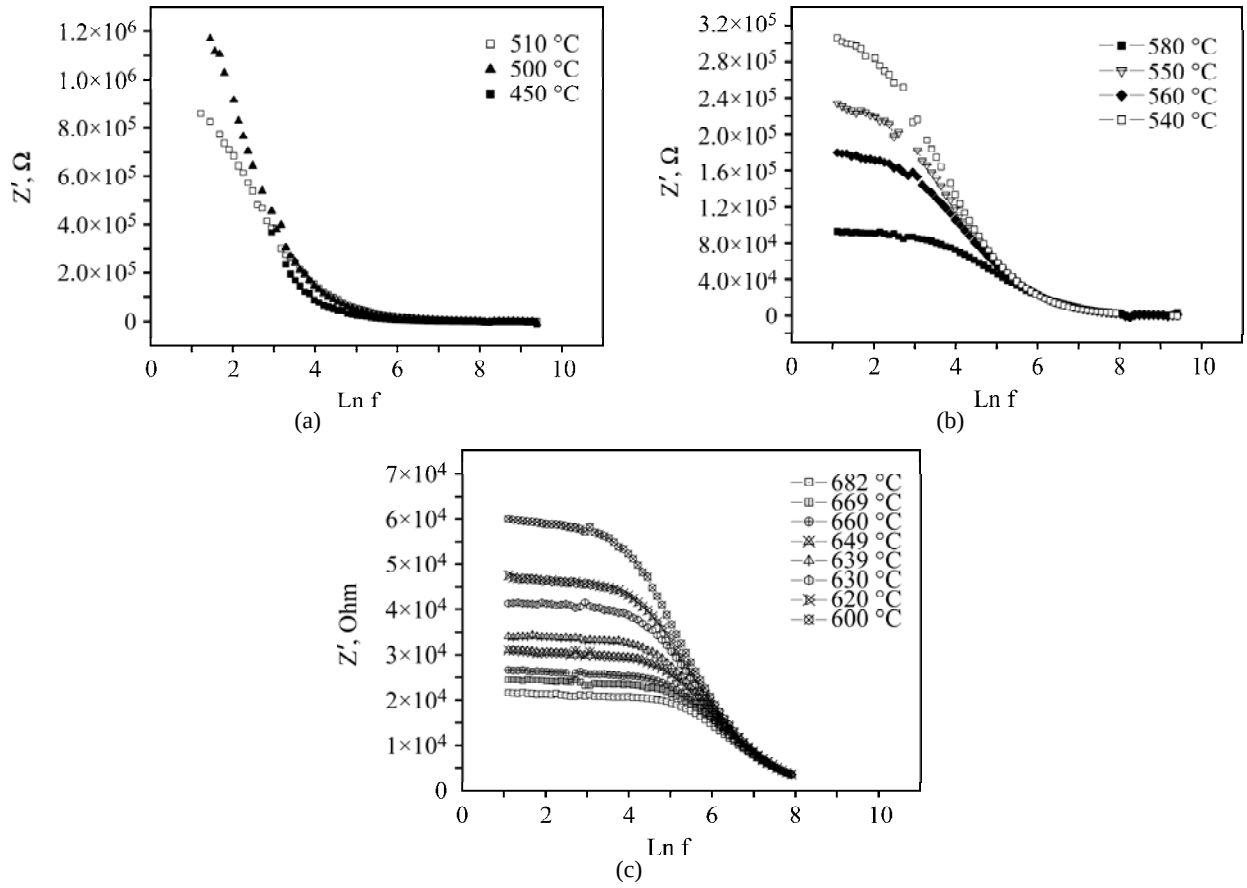

Fig. 5. Variation of real part of impedance (Z') as a function of frequency for illite It-1 sample.

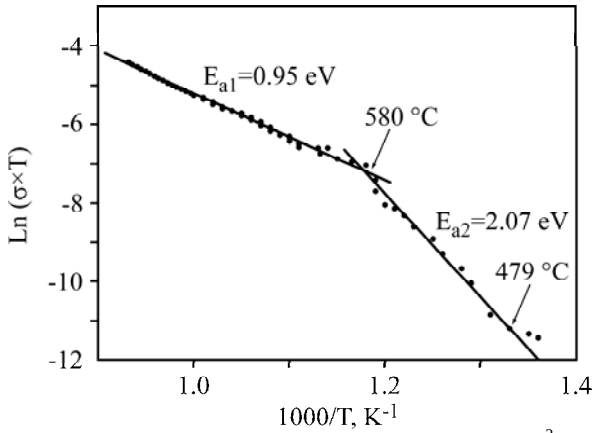

Fig. 6. Variation of σ(ω) (bulk conductivity) against $10^3/T$ K^{-1} for illite It-1.

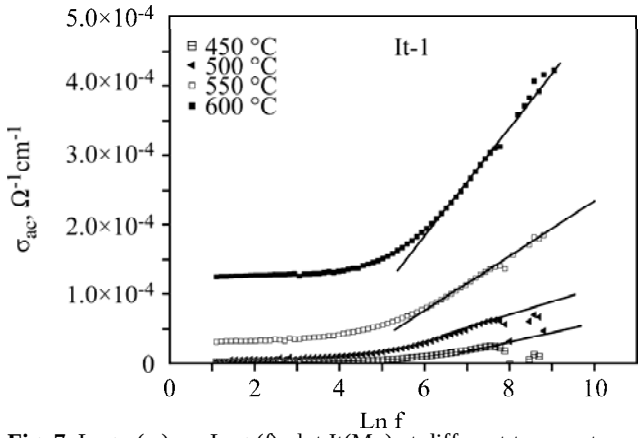

Fig. 7. Log σ(ω) vs. Log (f) plot It(Mo) at different temperatures (450–800°C) for It-1.

According to Jonscher (1977) [29], the origin of the frequency dependence of conductivity lies in the relaxation phenomena arising due to mobile charge carriers.

Figs. 8 shows the variation of real part of electric modulus M' as a function of frequency at different temperatures. At lower frequencies, M' tends to be very small confirming that the electrode effects make a negligible contribution and hence may be ignored when the data are analyzed in modulus formalism [25]. In the figure M' reaches to constant value $M\infty$ at high frequencies for all temperatures and this due to relaxation processes, which are spread over a range of frequencies.

The variation of M'' with frequency is shown in Fig. 9 at different temperatures. In the M'' plot; the peaks are broader and asymmetric on both sides of the maxima than predicted by ideal Debye behavior. The frequency range where the peaks occur is indicative of transition from long range to short-range mobility [25, 30]. The peak in the M'' plot shifts tower higher frequencies with increase in temperature and also the peak height increases. The high frequency side of the M'' peak represents the range of frequencies in which the ions are spatially confined to their potential wells. The peak frequency of the pattern, corresponding to maximum value of M'' is called conductivity relaxation frequency, gives an

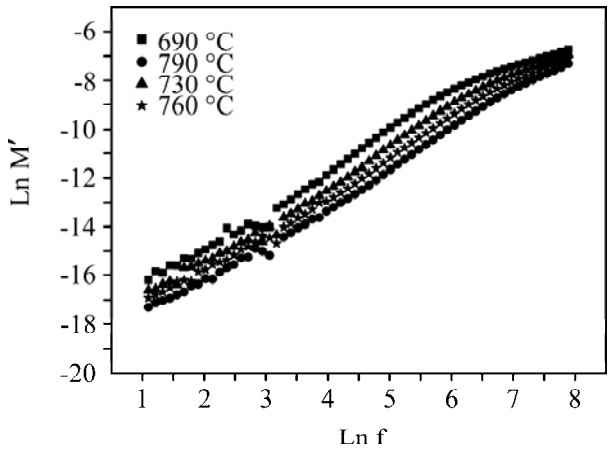

Fig. 8. Variation of real part of electrical modulus (*M*') as a function of frequency for illite It-1.

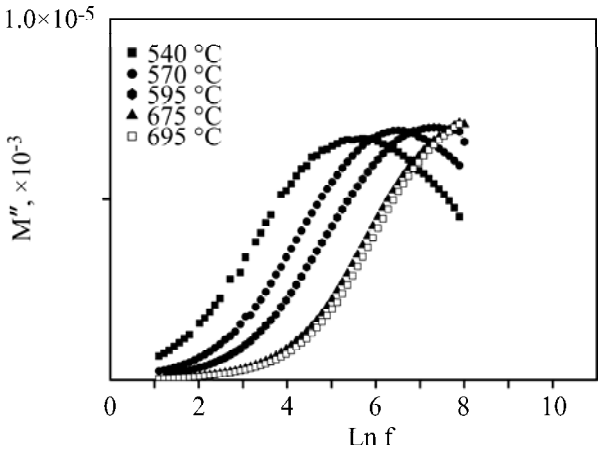

Fig. 9. Variation of imaginary part of complex modulus (*M*") as function of frequency at different temperatures for illite It-1.

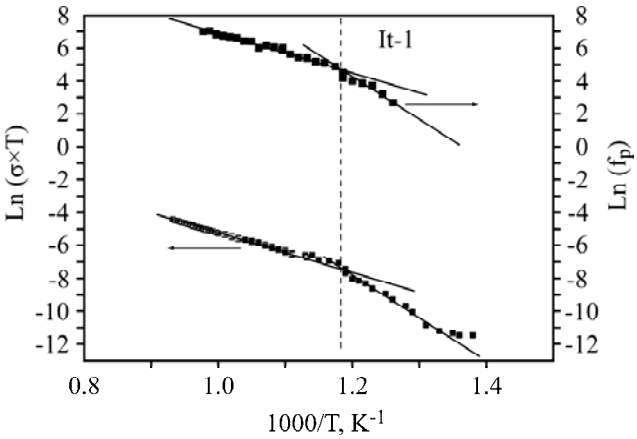

Fig. 10. Comparison of the Variation of Ln σ and Ln f_p as a function of temperature for the illite It-1.

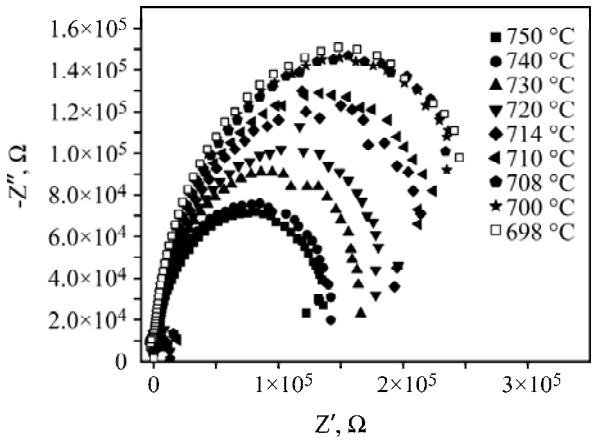

Fig. 11. Impedance spectrum of kaolinite Ha-Kass as a function of temperature.

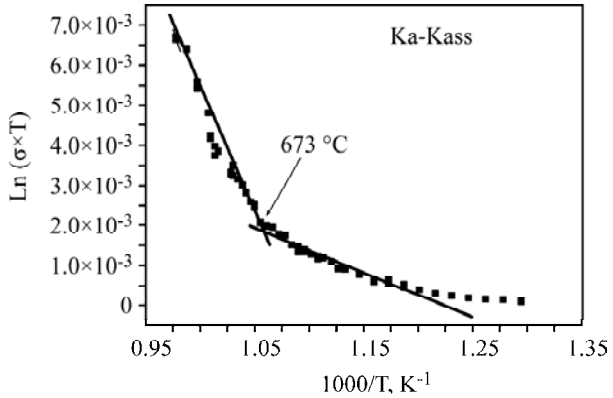

Fig. 12. Variation of σ(*ω*) as a function of temperature for halloysite sample (Ha-Kass).

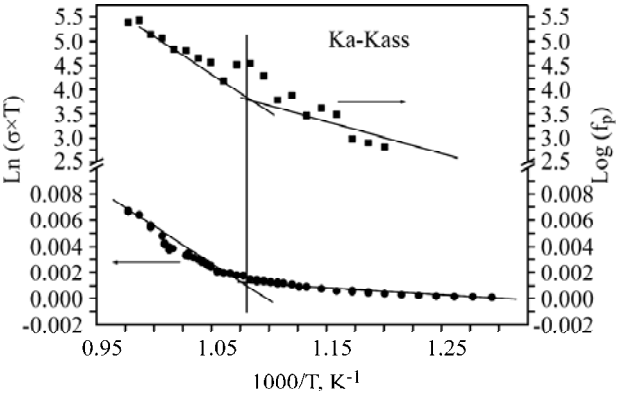

Fig. 13. Comparison of the variation of Ln (σ × *T*) and Ln f_p as a function of temperature for halloysite sample Ha-Kass.

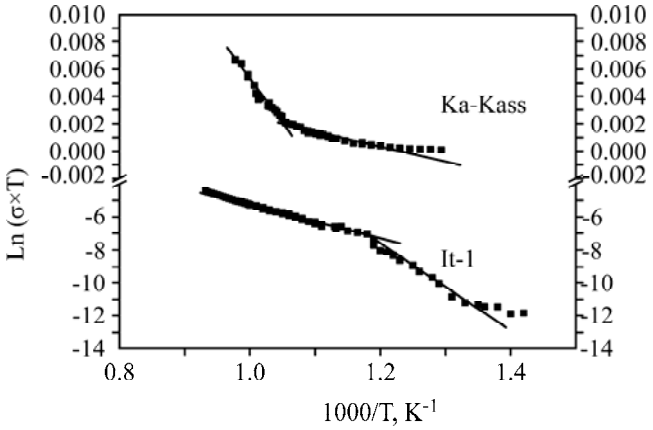

Fig. 14. Comparison of variation of Ln (σ × *T*) vs 1000/*T* as a function of temperature for halloysite Ha-Kass and illite It-1 samples.

estimate of conduction relaxation time (τ) in accordance with the relaxation $\omega_{max}\tau_\sigma = 1$. The value of relaxation frequency has been calculated in the temperature range (182–800°C) and its variation as a function of temperature is shown in Fig. 10.

The variation of $Ln\ f_{max}$ as a function of inverse absolute temperature appears to be linear satisfying the relation $f_p = f_{po} \exp(-E_f/kT)$. We can also note that experimental points representing simultaneously the variations of conductivity and frequency f_p with temperature are located on segments of parallel lines leading to the same slope values. Therefore, the activation energy values estimated from the AC conductivity pattern and modulus pattern are very similar and suggest the possibility of long-range mobility of charge carriers (ions) via hopping mechanism at higher temperature. Further, the appearance of peak in the modulus spectrum provides a clear indication of conductivity relaxation.

On the other hand, a similar study has been conducted on halloysite clay sample (Ha-Kass) in order to compare the ionic conduction mechanism in these materials of different structural properties. Impedance spectrum results indicate only the presence of a single semicircular arc whatever the temperature considered and hence the electrical processes in the material may be attributed to only intragrain phenomena (Fig. 11), which is not the case for illite It-1. The existence of a temperature-dependent electrical relaxation phenomenon in Ha-Kass sample has been also observed (variation of imaginary part of impedance (Z'') as a function of frequency). In addition, as observed in It-1 the analysis of impedance spectra in the low frequency region, show a decrease in the magnitude of Z' with rise in temperature i.e. negative temperature coefficient of resistance (NTCR)-type behavior like that of semiconductors.

The AC conductivity σ(ω) analysis shows typical Arrhenius behavior when observed as a function of temperature (Fig. 12). This curve indicates the presence of two different slopes in the pattern σ(ω) vs. $10^3/T$, located above and below 673°C, corresponding respectively to activation energy values $Ea_1 = 0.94$ eV and $Ea_2 = 4.93$ eV, which ascribe very likely to a modification of the structural material. Indeed, during this temperature 550–680°C a dehydroxylation process of the clay occurs and kaolinite forms metakaolinite by dehydroxylation [31].

On the other hand, the possibility of long-range mobility of charge carriers (ions) via hopping mechanism at higher temperature requires a comparison of activation energy value estimated from conductivity σ(ω) and modulus pattern ($\mathrm{Ln}f_p$) as function of temperature. Indeed, the variation of $\mathrm{Ln}\ \sigma T$ and $\mathrm{Ln}f_p$ as a function of inverse of temperature is representing simultaneously as a comparison in Fig. 13. A non-similarity in the of activation energy values is evident from these plots due to the obtaining of different slope values. Consequently, this finding can confirm that the ionic conduction mechanism in the Ha-Kass is not of type hopping as in the case of the illitic clay sample. This significant difference indicates that two phenomena or a mixture of several phenomena is measured simultaneously for the material. An electrical charge transport has been demonstrated in the investigated sample and it is very likely that the charge transport is mainly of electronic nature.

Discussion concerning the electrical conductivity results of the studied clays

A comparative study of electrical conductivity has been conducted to better understand the electrical transport mechanism. Fig. 14 shows the variation of Ln ($\sigma \times T$) *vs* 1000/*T* for the two clay mineral samples.

According to our results, it appears clearly that electrical conductivity of the 1:1 halloysite clay sample, has a much higher electrical conductivity value than 2:1 illite It-1, there is about a factor 1000 between the values of conductivity regardless of the temperature considered (example at 727°C, $\sigma_{Ha\text{-}Kass} = 10^{-3}\ \Omega^{-1}\cdot cm^{-1}$, $\sigma_{It\text{-}1} = 5{,}4\times10^{-6}\ \Omega^{-1}\cdot cm^{-1}$). This electrical conductivity is probably closely related (i) to the microstructural of the clay mineral. In all cases, the values remain below 1 which is consistent with the works of Kaya, 1999 [32]. The author noted that normalized electrical conductivity values are < 1 for kaolinite of Georgia and > 1 for bentonite, determined at various water contents and NaCl concentrations; (ii) to the dimensions of the cell that seem to play an important role in the mobility of the charge carriers (cations) present in the interlayer spacing of illite and kaolinite samples. From our point of view, the decrease of electrical conductivity of illite with respect to halloysite, is mainly related to the structure of this mineral. It is well known that illite is a 2:1 clay mineral with potassium (K) in the interlayer that restricts shrinking and swelling. Potassium ions bind to the oxygen plane of the basal tetrahedral layer of adjacent units and are not exchangeable ions. The displacement of cations (mainly Na^+ ions which are mobile than other cations in interlayer spacing is slowed by the presence of K^+ ions of greater size creating a steric blocking effect and therefore, the activation energy of the motion process increases resulting in a decrease of the ionic conductivity. Moreover, the presence of K^+ ions can alter the distribution of Na^+ in the different available sites. The conductivity may also decrease due to decrease of the number of mobile ions. About halloysite, things are otherwise, it has one layer of silicon atoms and one layer of aluminum layers in 1:1 structure. It is non-expanding clay mineral and dif-

ferent layer are held together by hydrogen bonding which occurs between the plane of basal oxygen atoms within a tetrahedral sheet and the plane of hydroxyl group within the octahedral layer. In the case of halloysite sample, the mobility of cations (essentially Na^+ ions in the interlayer) is high leading to a decrease of the activation energy of the motion process and subsequently to an increase of the ionic conductivity. In any case, more studies are necessary to clarify these points and to locate the Na^+ ions in the structure of these clay minerals.

CONCLUSION

The electrical conductivity measurements performed on the two clay minerals show that the mobility of the cations in interlayer spacing (mainly Na^+) is mostly influenced by the structure of these materials. In illite sample, some Na^+ ions are less mobile, due to the presence of K^+ ions, leading to a decrease in the number of species participating in the conduction process which explains the decrease of ionic conductivity of this clay mineral when compared to kaolinitic sample.

REFERENCES

1. Arulanandan K. Dielectric Method for Prediction of Porosity of Saturated Soil. *J Geotech Eng-ASCE*. 1991, **117**, 673–683.
2. Robinson D.A., Bell J.P. and Bachelor C.H. The Influence of Iron Minerals on the Determination of Soil Water Content Using Dielectric Techniques. *J Hydrol.* 1994, **161**, 169–180.
3. Ficai, C. Caractéristiques des matières argileuses établies en mesurant les constantes et les pertes diélectriques dans le domaine de fréquence compris entre 30 kHz et 3 MHz. *Bull Soc Franc Ceram*. 1959, **42**, 7–16.
4. De Lima O.A.L. and Sharma M.M. A Generalized Maxwell-Wagner theory for Membrane Polarization in Shaly Sands. *Geophys.* 1992, **57**, 431–440.
5. Knoll M.D. *A Petrophysical Basis for Ground-penetrating Radar and Very Early Time Electromagnetic, Electrical Properties of Sand-clay Mixtures*. Ph.D. Thesis, University of British Columbia. 1996, 316 p.
6. Wildenschild D., Roberts J.J., and Carlberg E.D. Electrical Properties of Sand/Clay Mixtures: the Effect of Microstructure. *SEG Int. Exposition and 69th Annual Meeting.* Houston, TX. 1999, October 31-November 5.
7. Bona N., Rossi E., Capaccioli S. Electrical Measurements in the 100Hz-10GHz Frequency Range for Efficient Rock Wettability Determination. *SPE Journ.* 2001, **6**(1), 80–88.
8. Börner F.D. Combined Complex Conductivity and Dielectric Measurements on Core. *Proc. of the 1997 Int. Symp. of SCA in Calgary*, 1997, SCA, paper No 9736, 1–10.
9. Muccillo E.N.S., and Kleitz M. Impedance Spectroscopy of Mg-partially Stabilized Zirconia and Cubic Phase Decomposition. *J Eur Ceram Soc.* 1996, **16,** 453–465.
10. Rodrigues C.M.S., Labrincha J.A., and Marques F.M.B. Monitoring of the Corrosion of YSZ by Impedance Spectroscopy. *J Eur Ceram Soc.* 1998, **18,** 95–104.
11. Steil M.C., Thevenot F. and Kleitz M. Densification of Yttria-stabilised Zirconia-impedance Spectroscopy Analysis. *J Electrochem Soc.* 1997, **1**, 390–398.
12. McCarter W.J., Garvin S. and Bouzid N. Impedance Measurement on Cement Paste. *J Mater Sci Lett.* 1988, **7**(10), 1056–1057.
13. Christensen B.J., Mason T.O., and Jennings H.M. Influence of Silica Fume on the Early Hydration of Portland Cements using Impedance Spectroscopy. *J Am Ceram Soc.* 1992, **75,** 939–945.
14. Christensen B.J., Coverdale R.T., Olseon R.A., Ford S.J., Carboczi E.J., Jennings H.M. and Mason T.O. Impedance Spectroscopy of Hydrating Cement-based Materials. *J Am Ceram Soc*. 1994, **77,** 2789–2804.
15. Macdonald J.R and Barsoukov E. *Impedance Spectroscopy. Theory. Experiment and Applications.* N.Y. Wiley & sons. 2005. pp. 1–27.
16. Orazem M.E., Tribollet B. *Electrochemical Impedance Spectroscopy.* John Wiley & Sons, Hoboken, New Jersey. 2008. Part I, Background, pp. 3–96.
17. Bergaya F., and Vayer M. CEC of Clays: Measurement by Adsorption of a Copper Ethylenediamine Complex. *Appl Clay Sci*. 1997, **12**, 275–280.
18. Brindley G.W., Brown G. *Crystal Structure of Clay Minerals and their X-ray Identification*. Mineralogical Society, London. 1980. 495 p.
19. Ingram M.D. Ionic Conductivity in Glass. *Phys Chem Glasses.* 1987, **28**, 215–234.
20. Irvine D.C., Sinclair A.R. West A.R. Electroceramics: Characterization by Impedance Spectroscopy. *Adv Mater*. 1990, **2**, 132–138.
21. Selvasekarapandian S., Vijaykumar M. The Ac Impedance Spectroscopy Studies on LiD_yO_2. *Mater Chem Phys*. 2003, **80**, 29–33.
22. Brahma S., Choudhary R.N.P., Thakur A.K. AC Impedance Analysis of $LaLiMo_2O_8$ Electroceramics. *Physica B.* 2005, **355**, 188–201.
23. Macdonald J.R. and Johnson W.B. *Fundamentals of Impedance Spectroscopy in Impedance Spectroscopy-Emphasizing Solid Materials and Systems*. 1987. Chap I, 1–26, John Wiley & sons, New York.
24. Chatterjee S., Mahapatra P.K., Choudhary R.N.P., Takur A.K. Complex Impedance Studies of Sodium Pyrotungstate-$Na_2W_2O_7$. *Phys Stat Sol. (a).* 2004, **201**, 588–595.
25. Sahoo P.S., Panigrahi A., Patri S.K. and Choudhary R.N.P. Impedance Spectroscopy of $Ba_3Sr_2DyTi_3V_7O_{30}$ Ceramic. *Bull Mater Sci.* 2010, **33**, 129–134.
26. Płocharski J. and Wieczorek W. Impedance Spectroscopy and Phase Structure of PEO-NaI Complexes.

Solid State Ionics. 1998, **28–30**(2), 979–982.

27. Grim R.E., and Rowland R.A. Differential Thermal Analysis of Clay Minerals and other Hydrous Materials. *Am Mineralogist.* 1942, **27**, 746–761, 801–818.
28. Joncher A.K. *Dielectric Relaxation in Solids*. Chesla Dielectric Press, London. 1983, 56–67.
29. Jonscher A.K. The Universal Dielectric Response. *Nature*. 1977, **267**, 673–679.
30. Khatri P., Behera B., Srinivas V., and Choudhary R.N.P. Complex Impedance Spectroscopic Properties of $Ba_3V_2O_8$ Ceramics. *Research Letters in Materials Science.* 2008, Article ID 746256, 5 pages doi:10.1155/2008/746256.
31. Chakravorty A.K. Application of TMA and DTA for Study of the Crystallization Behaviour of SiO_2 in the Thermal Transformation of Kaolinite. *J Therm Anal.* 1993, **39**, 289–299.
32. Kaya A. Electrical Spectroscopy of Kaolin and Bentonite Slurries. *Turk J Eng Environ Sci.* 2001, **25**, 345–354.

Received 10.10.12
Accepted 30.11.12

Реферат

Диаграммы импеданса по цепи переменного тока использовались для анализа электрических характеристик двух разновидностей глинистых минералов из Туниса – галлосита и иллита, с соотношением сеток 1:1 и 2:1, соответственно, в зависимости от температурного режима: 80–800°C. Реальная и мнимая части комплексного сопротивления представлены в виде следов полуокружностей на комплексной плоскости. За исключением иллита It-1, то есть второго из исследованных образцов глин, представленные диаграммы подтверждают наличие как объемного, так и зернограничного эффекта при температуре 600°C и выше. Отмечается, что объемное сопротивление материала понижается при повышении температуры. Данные спектроскопии импеданса свидетельствуют о диэлектрической релаксации, которая выпадает из уравнения Дебая. Как видно из диаграмм Найквиста, для обоих исследованных образцов – галлосита и иллита, характерен отрицательный температурный коэффициент сопротивления. В работе представлены результаты анализа объемного электрического сопротивления и энергии активации для обоих исследованных образцов. Для иллита It-1, значения энергии активации, определяемые с помощью диаграмм удельной проводимости по переменному току и абсолютного значения, очень близки. Это говорит о возможной долговременной подвижности носителей заряда (ионов) с использованием прыжкового механизма переноса электричества при более высоких температурах. С другой стороны, для образцов галлосита из города Кассерин (Тунис), с использованием анализа абсолютного значения, можно допустить, что процессы переноса электричества, весьма вероятно, имеют электронный характер. Частота релаксации соответствует уравнению Аррениуса, причем значения энергии активации несравнимы со значениями, найденными для удельной проводимости.

Ключевые слова: каолинит, иллит, прыжковый механизм, анализ полной проводимости, удельная электропроводность.